Paddy Water Environ (2015) 13:179–189
DOI 10.1007/s10333-014-0419-1

ARTICLE

Influence of saltwater wedges on irrigation water near a river estuary

Haisheng Liu · Natsuki Yoshikawa · Susumu Miyazu · Kouhei Watanabe

Received: 4 July 2013 / Revised: 21 December 2013 / Accepted: 14 February 2014 / Published online: 5 March 2014

Abstract Paddy fields irrigated using water from the Shinkawa River in Niigata, Japan, are subject to adverse effects associated with the occurrence of saltwater wedges in the river. The extent of saltwater intrusion in the river varies, depending on river discharge and tidal amplitude. In this study, field observations and numerical simulation of the Shinkawa River estuary were applied to ascertain the influence of saltwater wedges on paddy cultivation during the irrigation period. The saltwater wedge was surveyed using an echo-sounding profiling system (SC-3); results indicated that the longitudinal profiles of the saltwater wedge were 4.7 and 2.2 km from the river mouth sluice gate at the high water mark of spring tide and at the low water mark of neap tide, respectively. According to the vertical profiling using electrical conductivity (EC) meters at bridges crossing the river, there was a rigid interface between freshwater and saltwater with a thin halocline zone of approximately 0.25 m. These profiles were well reproduced by the one-dimensional, two-layer, unsteady flow model. The results of the model simulation and EC observation indicate that when the vertical position of the halocline rises to 1.2 m below the inlet of the water intake pumping station, the EC value rises sharply to 1,500 μs/cm, which is an unsuitable level for irrigation water. It is estimated that for about 23 % of the total irrigation period, pump operation is halted as a result of this mechanism.

Keywords Saltwater wedge · Acoustic profiling system · Numerical simulation · Halocline

H. Liu · S. Miyazu
Graduate School of Science and Technology, Niigata University, 8050 Ikarashi 2-Nocho, Nishi-ku, Niigata 950-2181, Japan

N. Yoshikawa (✉)
Institute of Science and Technology, Niigata University, 8050 Ikarashi 2-Nocho, Nishi-ku, Niigata 950-2181, Japan
e-mail: natsuky@agr.niigata-u.ac.jp

K. Watanabe
Kowa, 6-1 Shinko-cho, Chuo-ku, Niigata 950-8565, Japan

Introduction

Seawater intrusion renders river water unsuitable for agricultural use. Saltwater intrusion often occurs in the form of a "saltwater wedge," in which the upper layer of freshwater and the underlying layer of saltwater are highly stratified because of the density difference between saltwater and freshwater; freshwater then flows seaward, while saltwater flows landward (Farmer 1951; Keulegan 1966). The phenomenon is likely to occur near the estuaries of rivers draining into the Sea of Japan owing to its small tidal range. The predominant factors that influence the magnitude of saltwater intrusion are the amount of freshwater discharged from upstream and the level of the tides (Hanawa and Sugimoto 1980; Uncles and Stephens 1996; Chen 2004; Brockway et al. 2006; Liu et al. 2007; Ralston et al. 2010; Gong and Shen 2011). The lower the freshwater discharge and the higher the tidal level, the greater the length of the saltwater wedge. A rise in the vertical position of the halocline increases the chances of saltwater mixing with irrigation water, which may damage agricultural crops. Agricultural fields irrigated with water from the Shinkawa River in Niigata (Fig. 1) following the occurrence of a saltwater wedge, have experienced significant yield loss and deterioration in rice quality. Attempts to avoid saltwater in irrigation waters have been made by the

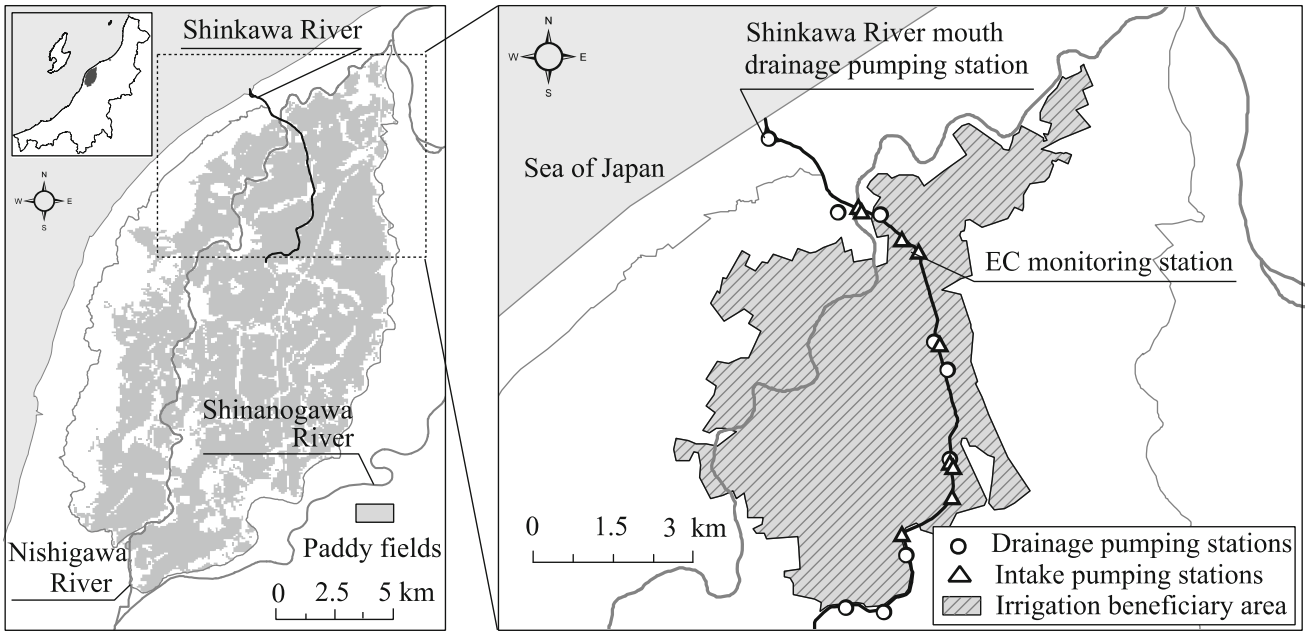

Fig. 1 Location of the study site

Water Management Office of this area. One such measure is the closure of the river mouth sluice gate near the river mouth when salinity, indirectly measured by electrical conductivity (EC), reaches an unallowable level (1,500 μs/cm) at the monitoring station 3.3 km upstream from the river mouth sluice gate. At this point, drainage pumps then drain saltwater out of the river. During periods when salinity is high, intake pumps along the river that supply irrigation water cease to operate.

However, this measure has some drawbacks. The operation of the drainage pumps is costly, and part of that cost is reimbursed by farmers. Regarding water balance, irrigation water becomes scarce and may be insufficient to meet the demands of the crops when high salinity is detected and intake pumps cease to run. Despite countermeasure efforts, the first class of rice harvested in the year 2010 made up only 10 % of the total rice production of this area. This was caused presumably by an insufficient irrigation water supply during a high water demand period due to halted operation of irrigation pumps under high-saline conditions.

A less expensive and more effective countermeasure is, therefore, needed; for example, a system that allows selective intake of freshwater. To develop such a countermeasure, the degree to which the saltwater wedge extends must be predicted. This study attempts to visualize the saltwater wedge in the Shinkawa River estuary by field observations and to evaluate the impact on irrigation water using a numerical model to simulate the behavior of the saltwater wedge during the irrigation period.

Materials and methods

Study area

The Shinkawa River collects drainage-water from agricultural and residential areas of the Nishikanbara district, which covers an area of 350 km^2 in the Niigata Plain, Japan. The topography of this district is characterized by a low-lying plain with approximately one-third of the land dipping below sea level. The Nishikanbara district is an alluvial plain created by the Shinano River, the longest river in Japan, and has fertile soil. Paddy production is the dominant land use, occupying about 198 km^2, or 57 % of the total area.

The total length of the Shinkawa River is approximately 15 km (Fig. 1). The mean discharge is about 24.0 m^3/s during the irrigation season, based on observations made between 2004 and 2010. The most important facility along the river is the river mouth drainage pumping station and sluice gate (Fig. 1). Its main purpose is to control floodwater, but it also functions to limit saltwater intrusion when saltwater is expected to exceed the level at which it would affect irrigation water. The Shinkawa River drains rainwater and drained water from paddy fields. The river water is also recycled as irrigation water in the downstream area because there is a shortage of irrigation water in the region. There are nine irrigation pumping stations along the river equipped to supply irrigation water (Fig. 1), having a beneficiary area of 33.3 km^2, which accounts for 17 % of the total paddy field areas in the district.

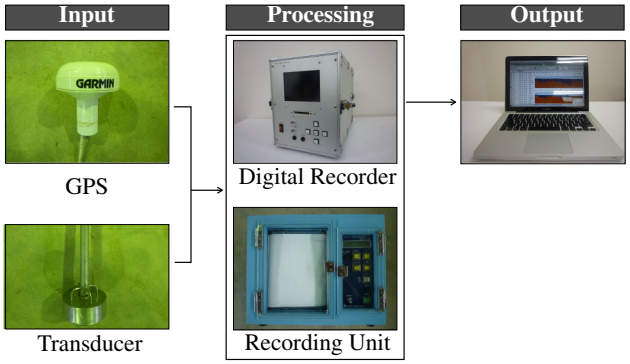

(a) System Composition

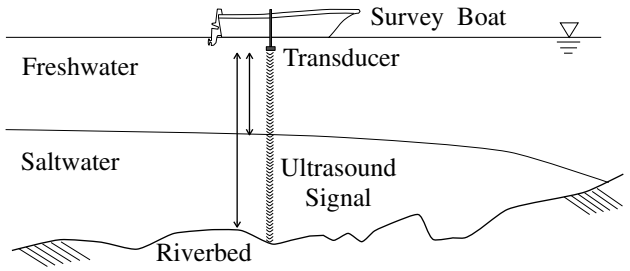

(b) Operation principle

Fig. 2 Acoustic profiling system: (**a**) System composition and (**b**) Operation principle

The river's estuary is characterized by an irregular semi-diurnal tide based on the sea level of the Niigata Nishiko port. The largest diurnal range of tide between flood tide and ebb tide was approximately 0.35 m in 2011 according to the tidal table of the Niigata Nishiko port. Because of this small tidal range, freshwater and saltwater are likely to be highly stratified, forming a saltwater wedge with a sharp vertical discontinuity in salinity.

Field surveys

Outline of an acoustic profiling system

Saltwater wedge observations were conducted using an echo-sounding system. The echo-sounding system, SC-3 (Senbon Denki Co. Ltd., Shizuoka, Japan) developed by Tokuoka et al. (2005) and Tateshi et al. (2006, 2007), consists of a recording unit, a digital recorder, a transducer, and a global positioning system (Fig. 2a). This system determines the longitudinal and cross-sectional position of the halocline by directing and receiving ultrasonic waves of 200 kHz to the riverbed from the transmitter fixed on a boat (Fig. 2b). The ultrasonic waves are reflected because of the density difference at the interface between freshwater and saltwater, and at the surface of the riverbed. The depths of the halocline and riverbed are determined based on the sound velocity and the time differences between the transmitted and reflected signals.

Table 1 Tide conditions of Niigata West Port on observation days

Position	Date	Condition	Time		Sea level (cm)
139.04 E 37.56 N	July 15, 2011	Spring tide	High water	13:29	48.9
			Low water	21:49	14.9
	August 23, 2011	Neap tide	High water	6:47	42.3
			Low water	16:21	25.9

Longitudinal saltwater wedge profiling using SC-3

To observe the variation in the longitudinal profile of the saltwater wedge under extreme conditions, we carried out two field surveys with the SC-3 targeting high water conditions at spring tide (July 15, 2011) and low water conditions at neap tide (August 23, 2011) (Table 1). Longitudinal profiling was implemented from the river mouth sluice gate, located at about 0.6 km from the actual Shinkawa river mouth, to the area furthest upstream of the saltwater wedge, about 4.7 km from the river mouth sluice gate along the center of the river.

Vertical profile of saltwater wedge using EC meters

Along with halocline profiling using SC-3, vertical profiling of salinity was carried out using EC meters CM-21P (DKK-TOA Corporation, Tokyo, Japan), which indirectly measure salinity. The vertical profiling was conducted at 10-cm intervals from the water surface to the riverbed at bridges crossing the Shinkawa River.

Velocity and flow direction of freshwater and saltwater layer

The velocities and flow directions of freshwater and saltwater were measured using electromagnetic current meters (INFINITY-EM, JFE Advantech Co. Ltd., Hyogo, Japan) for two tidal cycles (from September 29, 2011 to October 1, 2011). Two current meters were mounted 0.8 and 2.6 m off the riverbed and 1.88 km from the river mouth sluice gate to measure the velocity fluctuations of saltwater and freshwater. The depth of the river was 3.6 m, and the thickness of the saltwater layer was 2.0 m when the current meters were mounted at 8:00 on September 29, 2011. The interval between samples was 10 min.

Simulation

Numerical model

There are various numerical models capable of simulating saltwater intrusion into estuaries. Recently, two-dimensional, vertical, laterally integrated models, and three-dimensional models have been widely used to reproduce the spatial and temporal mixing processes of saltwater and freshwater under partially or strongly mixed conditions (Maccready and Geyer 2001; Liu et al. 2004; Zahed et al. 2008; Jeong et al. 2010; Gong and Shen 2011). In this study, the numerical model adopted is a one-dimensional, two-layer, unsteady flow model, originally developed by Suga (1977, 1979, 1981). The model was appropriate for this study because the condition of saltwater intrusion in the Shinkawa River is highly stratified and little mixture is observed. The critical output of this study is the vertical position of the halocline in comparison with the position of the inlets of water intake pumping stations, because the purpose of the numerical simulation is to evaluate the influence of the saltwater wedge on the intake of irrigation water.

Brief description of the model

The model contains the following six equations:

$$\frac{\partial h_1}{\partial t}+\frac{1}{B}\frac{\partial Q_1}{\partial x}=E \tag{1}$$

$$\frac{\partial h_2}{\partial t}+\frac{1}{B}\frac{\partial Q_2}{\partial x}=-E \tag{2}$$

$$\frac{\partial}{\partial t}(\rho_1 h_1)+\frac{1}{B}\frac{\partial}{\partial x}(\rho_1 Q_1)=\rho_2 E \tag{3}$$

$$\frac{\partial \rho_2}{\partial t}+u_2\frac{\partial \rho_2}{\partial x}=D_x\frac{\partial^2 \rho_2}{\partial x^2} \tag{4}$$

$$\frac{1}{g}\frac{\partial u_1}{\partial t}+\frac{\partial h_1}{\partial x}+\frac{\partial h_2}{\partial x}+\frac{u_1}{g}\frac{\partial u_1}{\partial x}+i_{f1}-i_0=0 \tag{5}$$

$$\frac{1}{g}\frac{\partial u_2}{\partial t}+\frac{\partial}{\partial x}(1-\epsilon)h_1+\frac{\partial h_2}{\partial x}+\frac{u_2}{g}\frac{\partial u_2}{\partial x}+i_{f2}-i_0=0 \tag{6}$$

where subscripts 1 and 2 denote the freshwater and saltwater layers, respectively, u is the flow velocity, Q is the discharge, ρ is the cross-sectionally averaged density of each layer, B is the river width, E is the saltwater entrainment coefficient, i_f is the friction slope, i_0 is the riverbed slope, ε is the relative density difference ($\varepsilon=(\rho_2-\rho_1)/\rho_2$), and D_x is the vertical diffusion coefficient (Fig. 3).

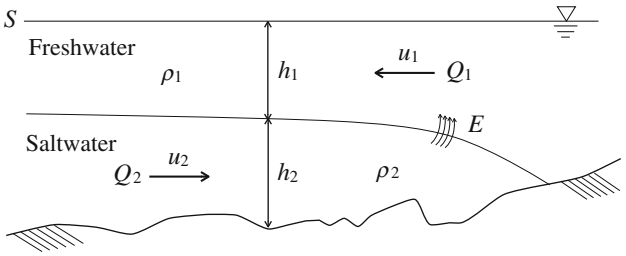

Fig. 3 Symbols in control equations

Equations (1) and (2) represent the volume conservation of the freshwater and the saltwater layer, Eq. (3) is a mass conservation of freshwater, Eq. (4) is a diffusion equation, and Eqs. (5) and (6) are the motion equations of freshwater and saltwater, respectively.

E, i_f and D_x are given as follows:

$$E=|u_1-u_2|2\times 10^{-3}F_1^3 \tag{7}$$

$$i_{f1}=\frac{f_i}{2gh_1}(u_1-u_2)|u_1-u_2| \tag{8}$$

$$i_{f2}=\frac{f_b}{gh_2}u_2|u_2|-\frac{f_i}{2gh_2}(1-\epsilon)\times(u_1-u_2)|u_1-u_2| \tag{9}$$

$$f_i=0.35\left(\mathrm{Re}_1F_1^2\right)^{-0.5} \tag{10}$$

$$D_x=5.93u_2^*h_2 \tag{11}$$

$$|u_2^*|=\sqrt{f_b u_2|u_2|-\frac{f_i}{2}(1-\epsilon)(u_1-u_2)|u_1-u_2|} \tag{12}$$

where f_i is the interfacial friction coefficient, f_b (=0.01) is the riverbed friction coefficient, F_1 and Re_1 are the densimetric Froude number and the Reynolds number of the freshwater layer, and u^*_2 is the shear velocity. Equation (7) and (8) are obtained based on the large-scale flume experiments and observation results of the Mogami River, Yamagata prefecture, Japan conducted by Suga and Takahashi (1975; 1976). Equation (11) is the equation used to calculate the vertical diffusion coefficient originally defined by Elder (1959).

For the sake of numerical calculation, terms with small order are ignored and the motion Eqs. (5) and (6) are transformed as follows:

$$\begin{aligned}\frac{\partial h_1}{\partial x}=\frac{1}{\phi}\Bigg[&-i_{f1}+i_{f2}-\epsilon F_2^2 i_0+\epsilon\left(1-F_1^2-\frac{u_1}{u_2}F_2^2\right)\frac{E}{u_1}\\&+\frac{u_1^2-u_2^2}{gB}\frac{\partial B}{\partial x}-\frac{h_1}{u_1\rho_2}\frac{\partial \rho_1}{\partial t}-\frac{\rho_1 h_1}{\rho_2^2}\frac{\partial \rho_2}{\partial x}+\frac{2u_1}{gh_1}\frac{\partial h_1}{\partial t}\\&-\frac{2u_2}{gh_2}\frac{\partial h_2}{\partial t}-\frac{1}{gh_1B}\frac{\partial Q_1}{\partial t}+\frac{1}{gh_2B}\frac{\partial Q_2}{\partial t}\Bigg]\end{aligned} \tag{13}$$

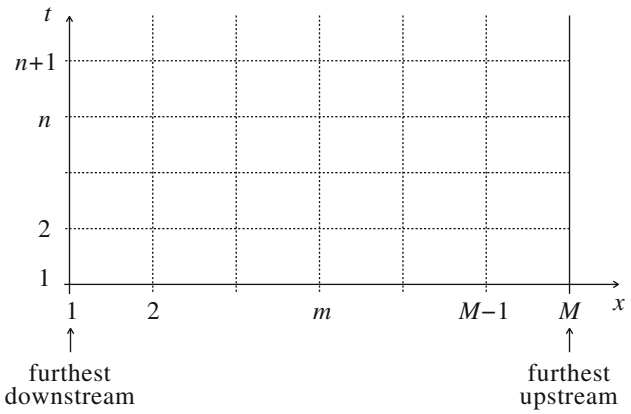

Fig. 4 Grid-points covering the computational domain and symbols

$$\frac{\partial h_2}{\partial x} = \frac{1}{\phi}\left[i_{f1} - i_{f2} + \epsilon(1 - F_1^2) i_0 - \epsilon\left(1 - F_1^2 - \frac{u_1}{u_2} F_2^2\right)\frac{E}{u_1} - \frac{u_1^2 - u_2^2}{gB}\frac{\partial B}{\partial x} + \frac{h_1}{u_1 \rho_2}\frac{\partial \rho_1}{\partial t} + \frac{\rho_1 h_1}{\rho_2^2}\frac{\partial \rho_2}{\partial x} - \frac{2u_1}{gh_1}\frac{\partial h_1}{\partial t} + \frac{2u_2}{gh_2}\frac{\partial h_2}{\partial t} + \frac{1}{gh_1 B}\frac{\partial Q_1}{\partial t} - \frac{1}{gh_2 B}\frac{\partial Q_2}{\partial t}\right] \quad (14)$$

$$\phi = \epsilon\left(1 - F_1^2 - F_2^2\right) \quad (15)$$

Within the extent that water surface is assumed to be horizontal, Eq. (14) is unnecessary since the depth of the saltwater layer (h_2) is automatically determined by provided the tide stage (S), the riverbed elevation and the depth of the freshwater layer (h_1).

Numerical solution

Numerical grid and symbols are defined as shown in Fig. 4. An implicit finite difference scheme was applied to discretize the Eqs. (1), (2), (3), (4), and (13). For example, the first term of the Eq. (1) can be discretized as follows;

$$\frac{\partial h_1}{\partial t} = \frac{1}{2\Delta t}\left(h_{1m}^{n+1} - h_{1m}^{n} + h_{1m-1}^{n+1} - h_{1m-1}^{n}\right) \quad (16)$$

where superscript n and subscript m denote timestep and grid-point number counted from downstream.

After discretizing all the terms in Eqs. (1), (2), (3), (4), and (13), the general forms of the discretized equations are finally transformed as follows:

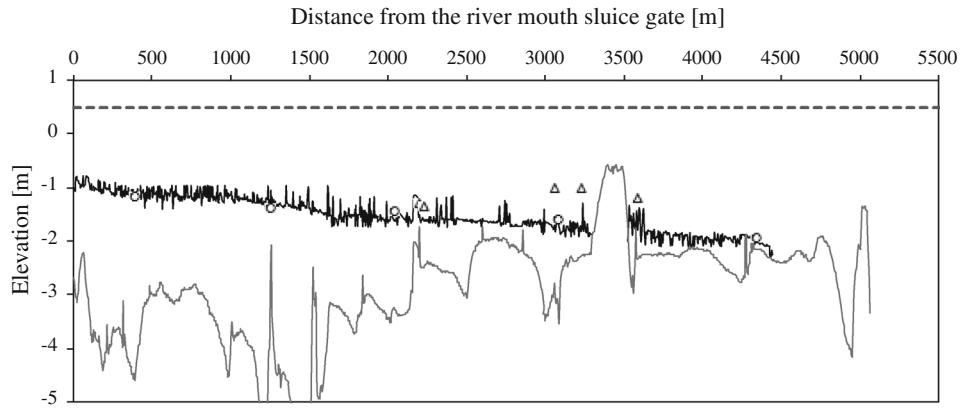

(a) Spring tide (July 15, 2011)

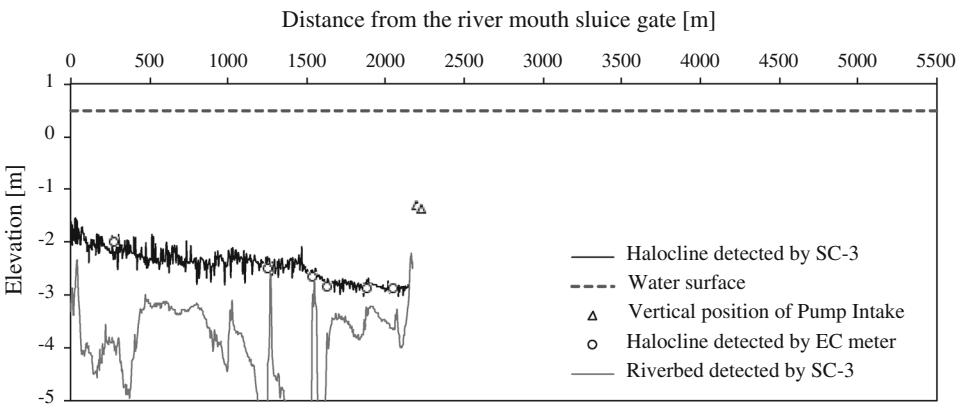

(b) Neap tide (August 23, 2011)

Fig. 5 The longitudinal profiles of saltwater wedge observed by SC-3 and EC meter: (**a**) Spring tide (July 15, 2011) and (**b**) Neap tide (August 23, 2011)

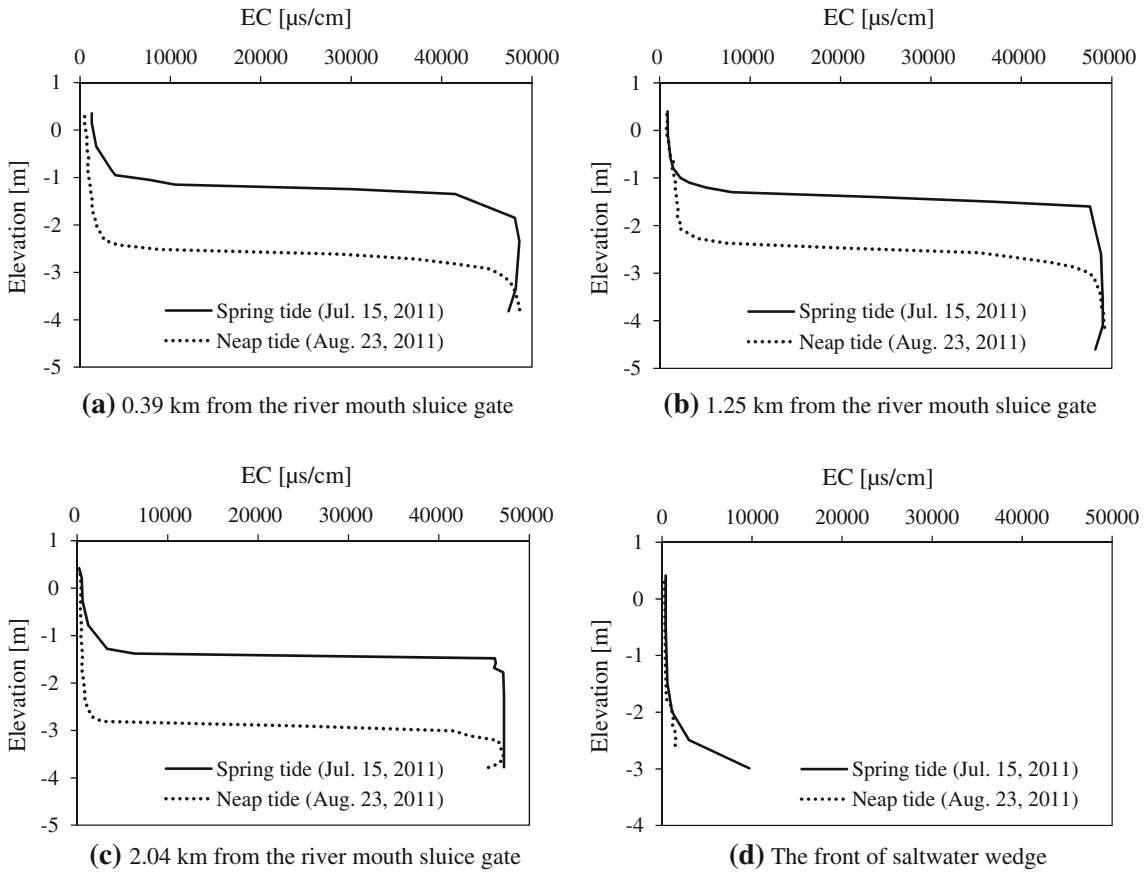

Fig. 6 The vertical salinity distributions at different positions: (**a**) 0.39 km from the river mouth sluice gate, (**b**) 1.25 km from the river mouth sluice gate, (**c**) 2.04 km from the river mouth sluice gate and (**d**) the furthest upstream of the saltwater wedge

$$a_{1m}h_{1m}^{n+1} + a_{2m}Q_{1m}^{n+1} + a_{3m}Q_{2m}^{n+1} + a_{4m}\rho_{1m}^{n+1} + a_{5m}\rho_{2m}^{n+1} = a_{6m} \tag{17}$$

$$a_{7m}Q_{1m-1}^{n+1} + a_{8m}Q_{1m}^{n+1} + a_{9m}h_{1m}^{n+1} + a_{10m}\rho_{1m}^{n+1} + a_{11m}\rho_{2m}^{n+1} = a_{12m} \tag{18}$$

$$a_{13m}Q_{2m-1}^{n+1} + a_{14m}Q_{2m}^{n+1} + a_{15m}h_{1m}^{n+1} + a_{16m}\rho_{1m}^{n+1} + a_{17m}\rho_{2m}^{n+1} = a_{18m} \tag{19}$$

$$a_{19m}\rho_{1m-1}^{n+1} + a_{20m}\rho_{1m}^{n+1} = a_{21m} \tag{20}$$

$$a_{22m}\rho_{2m-1}^{n+1} + a_{23m}\rho_{2m}^{n+1} = a_{24m} \tag{21}$$

where $a_1 - a_{24}$ are determinate values when all the variables one timestep before (n) are given.

To solve these equations, the following six boundary conditions are given: the downstream boundary conditions are depth of freshwater (h_1), the tide stage (S), and the density of the saltwater layer (ρ_2); and the upstream boundary conditions are the discharge of freshwater (Q_1) and saltwater (Q_2), and the density of freshwater (ρ_1). Longitudinal values of variables are also given as initial conditions when $n = 0$.

The first step is the calculation of $a_1 - a_{24}$, which are determined using the values of variables at the initial conditions $n = 0$, and those calculated one timestep before for $n \geq 1$. Then, ρ_1 and ρ_2 are calculated, by solving Eq. (20) from the furthest upstream grid-point, downstream, and Eq. (21) from the furthest downstream grid-point, upstream. Given longitudinal values of ρ_1 and ρ_2 and boundary conditions, h_1 at the furthest upstream (h_{1m}^{n+1}) is calculated by Eq. (17), then Q_1 and Q_2 at one grid-point downstream (Q_{1m-1}^{n+1}, Q_{2m-1}^{n+1}) by Eqs. (18) and (19), respectively. The values of h_2 are determined as a difference between the total water depth and freshwater depth h_1. By repeating this procedure, all the longitudinal values are calculated, and then repeated for the next timestep.

Model application

To apply the model to the study river, the computational domain was set from the river mouth sluice gate to 15 km upstream, a distance at which no saltwater intrusion occurs. The computational domain was divided into 150 sections

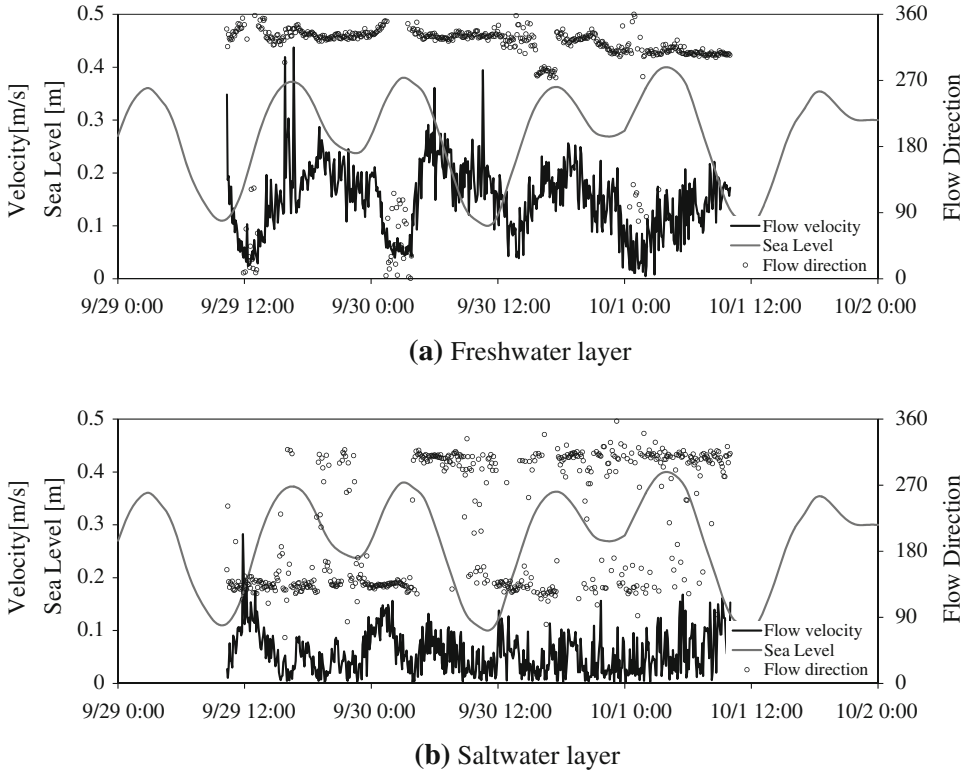

Fig. 7 The observed flow velocities and directions of (**a**) freshwater and (**b**) saltwater

of 100 m each. The model bathymetry and river width are based on the drawing of longitudinal sections and cross-sectional profiles obtained from the Water Management Office. The riverbed profile obtained by SC-3 was not applied because of the difficulty encountered in the numerical calculation when an abrupt change in the riverbed occurs. The time interval was 300 s.

The downstream boundary value of ρ_2 was assumed to be constant at 1.025 kg/m^3 based on field observations. The downstream boundary value of h_1 was determined by the function of river discharge. The value of S was given by the time series data with a 10-min interval provided by the Water Management Office. The value of h_2 was determined as the difference between S and h_1. The value of ρ_1 at furthest upstream was assumed to be constant at 1.00 kg/m^3 according to the values obtained indirectly by measuring the EC of the freshwater supplied from upstream. The time-series data of Q_1 supplied from the upstream area were obtained from the Water Management Office. The Q_2 at the furthest upstream point was set at 0 m^3/s because the saltwater wedge did not reach that point.

In addition to the freshwater supplied from the furthest upstream point, the freshwater volume varies as a result of the operation of nine intake pumping stations and ten drainage pumping stations within the computational domain. The intake and discharge volumes of these pumping stations were incorporated in the model as positive and negative lateral flows, respectively. The time-series data of pump operation were provided by the Water Management Office.

Results

Survey results

Result of the longitudinal profile of saltwater wedge

Spring tide (July 15, 2011) The maximum and minimum tidal levels on July 15, 2011 were 0.49 m and 0.15 m, respectively. The average river discharge supplied from upstream (Q_1) during the observation period (10:00–13:00) was 18.9 m^3/s. The average river discharge near the river mouth sluice gate during the observation period was 38.7 m^3/s.

Figure 5a shows the longitudinal profile of the saltwater wedge under the conditions of spring tide, with the horizontal and vertical positions of inlets of intake pumping stations overlaid. The length of the saltwater wedge extended about 4.7 km from the river mouth sluice gate around the high water mark of spring tide. Five out of nine intake pumping stations were within the longitudinal range of the saltwater wedge. The intake pumping station located about 2.6 km from the river mouth sluice gate had its inlet as low as −1.36 m, and the halocline elevation was about −2.07 m from the surface of the water. The difference in depth was 0.71 m.

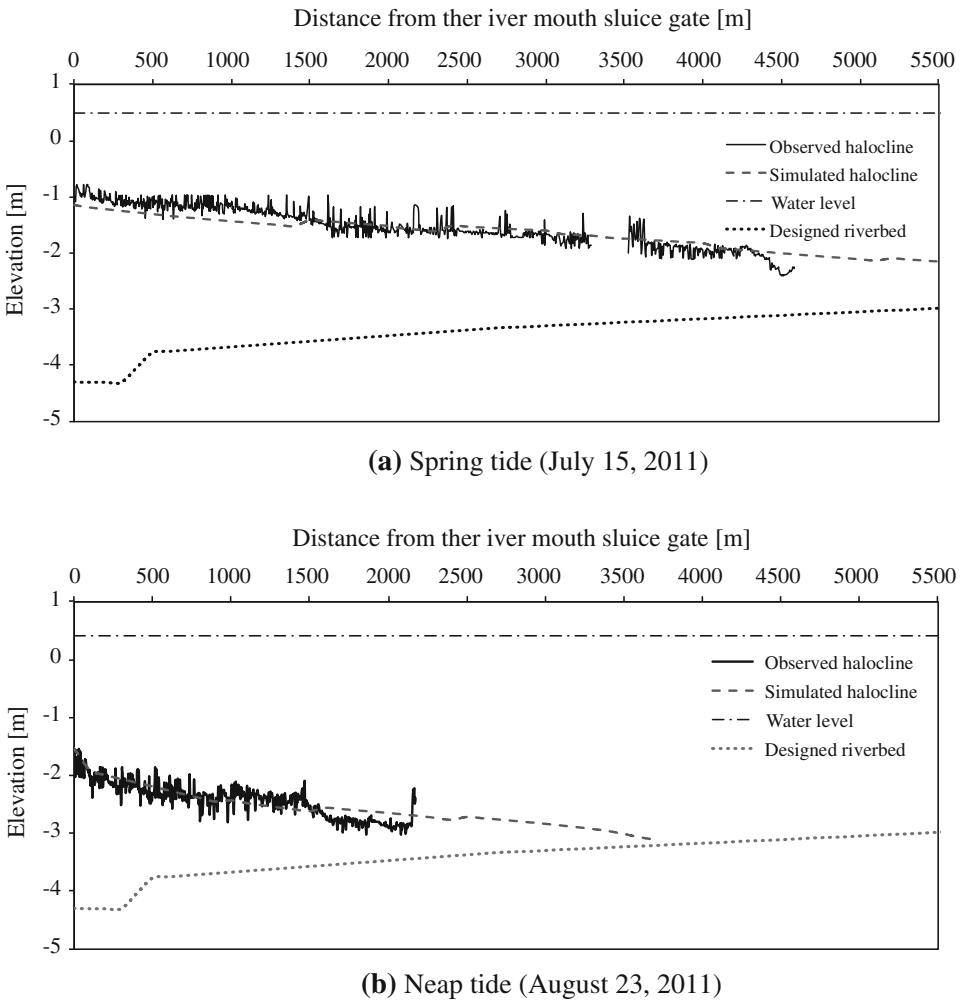

Fig. 8 Longitudinal halocline profiles by observation and numerical simulation in the case of (**a**) spring tide and (**b**) neap tide

Neap tide (August 23, 2011) The maximum and the minimum tidal levels on August 23, 2011 were 0.42 and 0.26 m, respectively. The average river discharge of the furthest upstream point during the observation period (15:00–16:00) was 10.3 m^3/s, and discharge near the river mouth sluice gate was 35.4 m^3/s.

Figure 5b shows the longitudinal profile of the saltwater wedge under the conditions of a neap tide. The saltwater wedge was about 2.2 km from the river mouth sluice gate around the low water mark. Compared with the spring tide condition, the saltwater wedge was approximately 2.5 km shorter and 0.80 m thinner on average. There were no intake pumping stations in the longitudinal extent of the saltwater wedge.

Vertical profile of saltwater wedge

Figure 6a–c show the vertical EC profiles measured at 0.39, 1.25, and 2.04 km upstream from the river mouth sluice gate, respectively. In the cases of both spring and neap tides, the abrupt change in EC between the freshwater and saltwater layers with an average halocline of 0.25 m suggests the existence of a fairly stable saltwater wedge. As shown in Fig. 6d, while the saltwater wedge was not present 2.19 km upstream from the river mouth sluice gate during a neap tide, the saltwater wedge was present at that point during a spring tide.

The vertical positions of the halocline measured by the EC meters along the river are overlaid in Fig. 5. The halocline center was defined to be 20,000 μs/cm. These results demonstrate that the SC-3 successfully captured the longitudinal profile of the halocline.

Velocity of freshwater and saltwater

Figure 7 shows the velocities and directions of freshwater and saltwater observed by the current meters between September 29 and October 1, 2011 (two tidal cycles). The velocity of freshwater shown in Fig. 7a fluctuated between 0.005 and 0.437 m/s with the tidal level variation; the velocity tended to become smaller during the flood tide period, and larger during the ebb

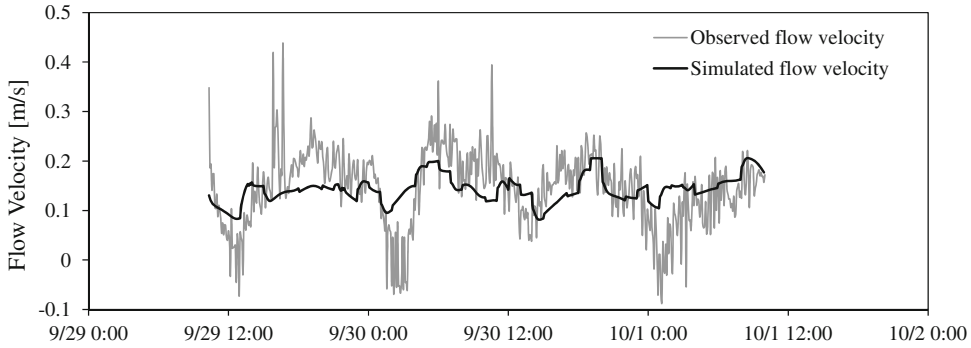

(a) Freshwater layer

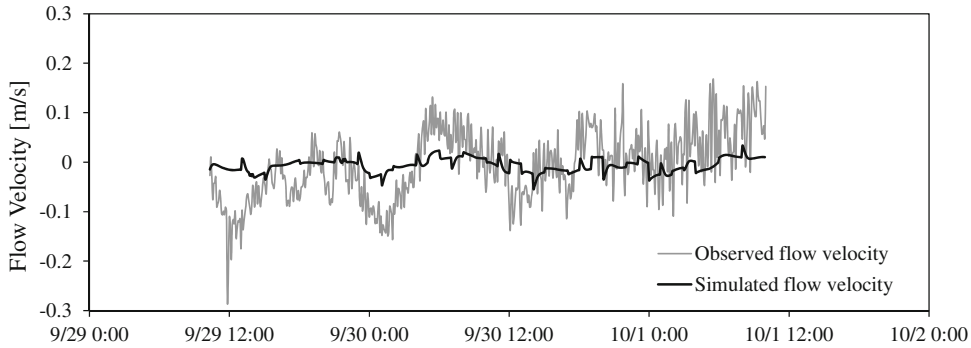

(b) Saltwater layer

Fig. 9 The velocities of freshwater and saltwater by observation and numerical simulation : (**a**) Freshwater layer and (**b**) Saltwater layer

tide period. The flow directions were mostly northwest, that is seaward, during the period of flood and ebb tides except for the short periods around low and high water conditions.

Variation in the velocity of underlying saltwater shown in Fig. 7b was between 0.001 and 0.282 m/s, with an average of 0.057 m/s. The flow direction of the saltwater layer was more sensitive to the tidal movement than that of freshwater. During the observation period, 43.6 % of flow was seaward and 51.8 % was landward.

Calculation results

The distribution of the saltwater wedge

Figure 8 shows the simulated saltwater wedge intrusion on July 15 and August 23 compared with that observed in the field. Halocline elevations were reproduced well in both cases. However, the longitudinal extent of the simulated saltwater wedge on July 15 was about 1 km longer, and on August 23 was about 1.3 km longer than the observed extent. The difference was due to mainly the adoption of a smoother riverbed profile based on the drawing of the longitudinal section in the model, though the actual bathymetry of the river is fairly rough. Because the purpose of this study is to evaluate the influence of the saltwater wedge on agricultural water intake, the relative vertical position of the density interface needs to be accurately simulated, while the longitudinal extent is less important.

Velocity of saltwater and freshwater

The calculated velocities of freshwater and saltwater during the survey period are shown in Fig. 9. Positive values indicate seaward flow, and negative values indicate landward flow. The calculated range of fluctuation is smaller than the observed range for both freshwater and saltwater layers. This may be caused by the influence of wind, which is not accounted for in the model. The calculated flow direction and average velocities are fairly consistent with the observed values. The calculated and observed average velocities of freshwater were 0.144 and 0.141 m/s seaward, and those of saltwater were 0.058 and 0.064 m/s landward. These results demonstrate that the one-dimensional, two-layer, unsteady flow model can satisfactorily simulate the salinity intrusion in the Shinkawa River under a range of tidal level and river discharge conditions.

Simulation of saltwater wedge influence on agricultural water intake

Saltwater enters the irrigation channel through the inlet of the water intake pumping station. Therefore, the relative

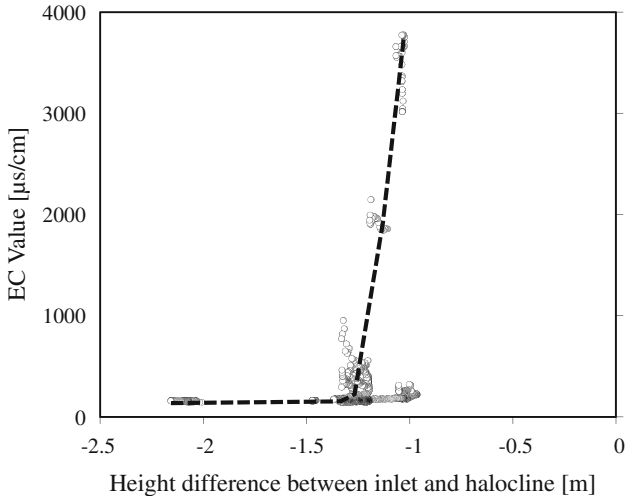

Fig. 10 Relationship between EC values observed at monitoring station (Nakasai intake pumping station) and relative halocline position to the inlet simulated by the model

vertical positions of the water intake pumping station inlets, and the halocline are the critical factors that determine the degree of saltwater mixing. Because the river mouth sluice gate closes when the EC value of the monitoring station at the Nakasai intake pumping station (Fig. 1) reaches 1,500 μs/cm, the behavior of the saltwater wedge and the extent of saltwater mixing without operation of the gate throughout an irrigation period are unknown. The model was used to simulate saltwater wedge behavior without the gate operation for the irrigation period in 2011.

The relationship between the vertical position of the halocline and the EC value observed at the Nakasai intake pumping station is shown in Fig. 10. EC values greater than 1,500 μs/cm are observed immediately before the countermeasure was practiced, and the height difference between the inlet and halocline is the simulated result. This result implies that when the vertical position of the halocline rises to 1.2 m below the inlet of the water intake pumping station, the EC value rises sharply at the unsuitable standard for irrigation water, 1,500 μs/cm. Since the EC value of the saltwater itself is about 45,000 μs/cm, even minor mixing of saltwater due to the suction generated by pumps makes the irrigation water unsuitable for irrigation use. According to the simulation result, this condition would occur for about 23 % of the irrigation period if the countermeasures were not practiced.

Conclusions

Saltwater wedge intrusion was investigated by the field observations and numerical simulations in the estuary of the Shinkawa River. As indicated by longitudinal and vertical profile visualization, the saltwater wedge in the Shinkawa River moves into the estuary at each tidal event with strong stratification, causing salinization of irrigation water. Since the vertical position of the halocline is the determining factor of the extent of the mixing of saltwater with irrigation water, the present countermeasure, closing the river mouth sluice gate in combination with discharging the river water by pumps, is effective to lower the position of the halocline and to avoid the intrusion of high-salinity water into irrigation water. However, operation of the drainage pumps is costly, and this countermeasure brings about a shortage of irrigation water because the water intake pumping stations cease operation. In drought years in particular, the frequency and magnitude of saltwater intrusion increases because of a lower freshwater supply from upstream; this is problematic because of the higher water demand to supplement high rates of evapotranspiration during these times. Therefore, more effective and efficient countermeasures to lower the vertical position of the halocline must be introduced. We are currently developing proposals for several alternative countermeasures, such as increases in the volume of freshwater supply in the river by manipulating the operation timing of the drainage pumps equipped further upstream than the longitudinal profile of the saltwater wedge, or controlling the sluice gate openness to eliminate only the saltwater layer out of the river with only a head difference between inside and outside the gate. These proposals will be tested in situ, and, if successful, will help alleviate the costs associated with operation of the river mouth pump, and allow for continuous intake of irrigation water.

Acknowledgments We are grateful for experiment support from the Ministry of Agriculture, Forestry and Fisheries, Ministry of Land, Infrastructure, Transport and Tourism, Niigata Prefectural Government, and Nishikanbara Water Management Office of Niigata city, Japan. We are also grateful to the Niigata University and the China Scholarship Council.

References

Brockway R, Bowers D, Huguane A, Dove V, Vessele V (2006) A note on salt intrusion in funnel-shaped estuaries: application to the Incomati Estuary, Mozambique. Estuar Coast Shelf Sci 66:1–5

Chen XJ (2004) Modeling hydrodynamics and salt transport in the Alafia River estuary, Florida during May 1999–December 2001. Estuar Coast Shelf Sci 61:477–490

Elder JW (1959) The dispersion of a marked fluid in turbulent shear flow. J Fluid Mech 5(4):544–560

Farmer HG (1951) An experimental study of salt wedges. Woods Hole Oceanographic Institution, Woods Hole, pp 3–4

Gong W, Shen J (2011) The response of salt intrusion to change in river discharge and tidal mixing during the dry season in the Modaomen Estuary, China. Cont Shelf Res 31:769–788

Hanawa K, Sugimoto T (1980) Effect of the variation of river discharge on flushing and recovery of salt wedge (2). J Tôhoku Geophys 27(1):1–17

Jeong S, Yeon K, Hur Y, Oh K (2010) Salinity intrusion characteristics analysis using EFDC model in the downstream of Geum River. J Environ Sci (China) 22(6):934–939

Keulegan GH (1966) The mechanism of an arrested saline wedge. In: Estuary and coastline hydrodynamics. McGraw-Hill, New York, pp 546–574

Liu WC, Hsu MH, Wu CR, Wang CF, Kuo AY (2004) Modeling salt water intrusion in Tanshui River estuarine system: case-study contrasting now and then. J Hydraul Eng 130:849–859

Liu WC, Chen WB, Cheng RT, Hsu MH, Kuo AY (2007) Modeling the influence of river discharge on salt intrusion and residual circulation in Danshuei River Estuary, Taiwan. Con Shelf Res 27:900–921

MacCready P, Geyer WR (2001) Estuarine salt flux through an isohaline surface. J Geophys Res 106:11629–11637

Ralston DK, Geyer WR, Lerczak JA (2010) Structure, variability, and salt flux in a strongly forced salt wedge estuary. J Geophys Res. doi:10.1029/2009JC005806

Suga, K, Takahashi A (1975) Interfacial friction coefficient of weakly mixed estuary. In: Proceeding of 30th annual meeting, JSCE, II, pp 470–471 (in Japanese)

Suga K (1977) Numerical calculation of one-dimensional and two layers unsteady flow. In: The 24th proceeding of coastal engineering, pp 544–548 (in Japanese)

Suga K (1979) Numerical calculation of one-dimensional and two layers unsteady flow. In: The 26th proceeding of coastal engineering, pp 567–571 (in Japanese)

Suga K (1981) Numerical calculation method of saline-wedge in tidal rivers. Civil Eng J 23–11:31–36 (in Japanese)

Suga K, Takahashi A (1976) Entrainment coefficient of density current flow. In: Proceeding of 31th annual meeting, JSCE, II, pp 383–384 (in Japanese)

Tateshi M, Honda Y, Tokuoka T, Fukita A, Anma K, Nishimura K (2006) Saline water intrusion into the Aganogawa River. Laguna 13:43–62 (in Japanese)

Tateshi M, Nguyen VL, Ta TKO, Tokuoka T, Fukita A, Nishimura K, Matsuda S (2007) Salt water intrusion in the Mekong River Estuary, Vietnam: observation at low flow season in May 2005. Sci Rep Niigata Univ E 22:57–78

Tokuoka T, Fukita A, Tateishi M, Nishimura K, Anma K, Matsuda S, Kawasumi T, Seki T (2005) Saline wedge observation by echo-sounding equipment (SC-3) and towing type water quality monitor (TPM CLOROTEC). Laguna 12:81–87 (in Japanese)

Uncles RJ, Stephens JA (1996) Salt intrusion in the Tweed Estuary. Estuar Coast Shelf Sci 43:271–293

Zahed F, Etemad-Shahidi A, Jabbari E (2008) Modeling of salinity intrusion under different hydrological conditions in the Arvand River Estuary. Can J Civ Eng 35:1476–1480